ELSEVIER

Journal of Molecular Catalysis B: Enzymatic 4 (1998) 219–227

JOURNAL OF MOLECULAR CATALYSIS B: ENZYMATIC

2-[(4″-Hydroxy-3′-methoxy)-phenoxy]-4-(4″-hydroxy-3″-methoxy-phenyl)-8-hydroxy-6-oxo-3-oxabicylo[3.3.0]-7-octene: unusual product of the soybean lipoxygenase-catalyzed oxygenation of curcumin

Claus Schneider [a], Alexander Amberg [a], Juliane Feurle [a], Andreas Roβ [a], Monika Roth [a], Gábor Tóth [b], Peter Schreier [a,*]

[a] *Lehrstuhl für Lebensmittelchemie, Universität Würzburg, Am Hubland, D-97074 Würzburg, Germany*

[b] *Technical Analytical Research Group of the Hungarian Academy of Sciences, Technical University Budapest, St. Gellert tér 4, H-1111 Budapest, Hungary*

Received 16 September 1997; accepted 17 October 1997

Abstract

Racemic (1*SR*,2*SR*,4*SR*,5*SR*)-2-[(4′-hydroxy-3′-methoxy)-phenoxy]-4-(4″-hydroxy-3″-methoxy-phenyl)-8-hydroxy-6-oxo-3-oxabicyclo[3.3.0]-7-octene (**2**, $C_{21}H_{20}O_8$) was isolated as major product of soybean lipoxygenase action on curcumin (**1**, $C_{21}H_{20}O_6$). The structure of **2** was elucidated by HPLC-APCI-MS and tandem MS, ^{1}H, ^{13}C, DEPT, H,H-COSY, H,C-HMQC, H,C-HMBC and phase sensitive 2D NOESY NMR techniques. For kinetic studies the rate of substrate degradation was followed spectrophotometrically at 430 nm, and the rate of oxygen consumption was measured polarographically. As evaluated by both methods, K_m for **1** was about four times higher than that obtained for linoleic acid (as the best substrate for soybean lipoxygenase); V_{max} was reduced five-fold. Lipoxygenase-mediated oxygenation of **1** was confirmed by the following criteria: (i) curcumin did not react with inactivated lipoxygenase; (ii) the enzymatic reaction was strongly inhibited by inhibitors such as BHA, deferoxamine and $HgCl_2$; (iii) oxygen consumption (measured polarographically) and curcumin degradation (measured photometrically) were shown to occur simultaneously at a ratio of 0.8 to 1, suggesting insertion of oxygen into **1** by lipoxygenase; (iv) molecular mass estimation by APCI-MS showed a shift of 32 in molecular mass from **1** (M_r 368) to **2** (M_r 400) being equivalent to an insertion of dioxygen. Curcumin meets none of the common features for lipoxygenase substrates and, therefore, may represent a new type of substrates for this enzyme.

Keywords: 2-[(4′-Hydroxy-3′-methoxy)-phenoxy]-4-(4″-hydroxy-3″-methoxy-phenyl)-8-hydroxy-6-oxo-3-oxabicyclo[3.3.0]-7-octene; Lipoxygenase; Curcumin; Dioxygenation

* Corresponding author. Tel.: +49-931-888-5481; fax: +49-931-888-5484.

1381-1177/98/$19.00
PII S1381-1177(98)00002-2

1. Introduction

Lipoxygenases (LOX) are nonheme-iron containing dioxygenases. They catalyze the insertion of molecular oxygen into polyunsaturated fatty acids [1,2]. Some LOX, e.g., soybean LOX-1 and LOX from tomatoes, exhibit a distinct regio- and enantioselectivity [3]. Common substrates, linoleic (18:2), linolenic (18:3) or arachidonic acid (20:4), containing at least one 1,4-*Z,Z*-pentadiene moiety, are oxidized to the corresponding chiral 2,4-*E,Z*-hydroperoxides. Only little is known about LOX substrates that differ from this pattern, i.e., ketoenoic acids [4,5] or 1,4-*Z,E*-pentadienes [6]. Oxygenation of other uncommon substrates such as carotenes [7] or retinoids [8] occurs via cooxidation, i.e., products are formed by action of intermediate fatty acid alkoxy and fatty acid peroxy radicals leading to unspecific oxidation [9,10].

In mammalian tissues, LOX catalyze the initial steps of the biosynthesis of physiologically active compounds such as leukotrienes and lipoxins [11]. The role of LOX in plants is less clear. They might be involved in seed germination, senescence and in plant wound response by formation of anti-pathogens, as well as compounds regarded as plant hormones [12–14].

Natural curcumin, a mixture of at least three related compounds (curcumin, demethoxy-curcumin, and bisdemethoxy-curcumin), is isolated from the rhizomes of *Curcuma longa* L., which have been reported to exhibit anti-inflammatory activity [15] and antiproliferative effects against human breast tumor cell lines [16]. Curcumin has been shown to have an inhibitory effect on mammalian 5-LOX and cyclooxygenase [17]. For further studies on the mechanism of anti-inflammatory properties of curcumin, a possible inhibitory effect on mammalian 15-LOX was investigated using soybean LOX-1 and linoleic acid as substrate [18]. Depending on its concentration, curcumin has been found to have a significant catalytic effect on the peroxidation of linoleic acid. This was inconsistent with results obtained with mammalian 5-LOX, but may be explained by different curcumin preparations used [18].

In our present study we show that soybean LOX-1 directly oxygenates curcumin as a substrate. The enzymatic nature of this oxygenation and the structure of the main product are described.

2. Materials and methods

2.1. Chemicals

Curcumin was synthesized according to the method described by Pabon [19]. Lipoxygenase (LOX, L-8383, Type I-S) was purchased from Sigma. BHA, deferoxamine, hydroquinone, dithizone were from Fluka, HPLC grade ethanol from Roth, solvents (diethyl ether and ethyl acetate) were of highest purity available and redistilled before use.

2.2. Photometric lipoxygenase assay

Ten mg of curcumin was dissolved in 4 ml of ethanol, then 6 ml of 0.1 M borate buffer (pH 8.0) was added. This stock solution was kept protected from light and was prepared freshly every day. Enzyme stock solution was prepared by dissolving 10 mg of LOX in 1 ml of buffer. Two milliliters of borate buffer (pH 8.0) and substrate (14–68 μM) were given in two cuvettes of the photometer. The reaction was started by adding 10 μl of enzyme solution into the blank cuvette. The decreasing absorbance at 430 nm in the blank cuvette due to degradation of curcumin resulted in a positive signal. The slope of the recorded curve was used to calculate the velocity (v) of the reaction. The molar absorbance coefficient ε of curcumin in 0.1 M borate buffer (pH 8.0) was determined to be 27,500 M^{-1} cm^{-1}.

The Michaelis–Menten parameters K_m and V_{max} were obtained by a Lineweaver–Burk plot as well as calculated using a computer

program (DNRPEASY, version 3.55, R.G. Duggleby/D.R. Leonhard, 1992).

Heat-inactivated LOX was obtained incubating the enzyme stock solution at 90°C for 10 min. For inhibitor studies the reaction was allowed to proceed for 1 min, then the inhibitor was added rapidly to the reaction mixture. All measurements were performed at ambient temperature (25°C) on a Shimadzu UV-2101 PC double beam spectrophotometer.

2.3. Polarographic lipoxygenase assay

All polarographic measurements were carried out using a Clark type oxygen electrode. Buffer (1 ml 0.1 M borate pH 8.0), substrate (27–270 μM) and inhibitors (see Table 2) were given into the cell; then the reaction was started by adding 10 μl of enzyme stock solution. The slope of the tangent laid onto the recorded curve was used to calculate the maximum velocity of the reaction.

2.4. Synthesis of acetylated curcumin

One hundred milligrams of curcumin was dissolved in 10 ml of dry pyridine, 10 ml of acetic anhydride was added and the mixture stirred under nitrogen for 24 h at room temperature. Remaining acetic acid anhydride was hydrolyzed by addition of 40 ml of ice-cold water and the solution was extracted three times with diethyl ether. The combined organic layers were washed three times with 0.1 M HCl and twice with water. After drying with Na_2SO_4 the solvent was evaporated and the residue was dissolved in ethanol. Acetylated curcumin was purified by preparative HPLC on a Lichrospher 100 NH_2 column (250 × 16 mm, 5 μm, 5 ml min^{-1}, Knauer, Berlin, Germany) with isocratic elution (EtOH/H_2O 85:15). The structure of the acetylated product was confirmed by ^{1}H-NMR (appearance of an additional 6-proton singlet at 2.48 ppm) and HPLC-MS analysis.

2.5. On-line liquid chromatography-tandem mass spectrometry (LC-MS/MS)

Mass spectrometry was performed on a Finnigan triple stage quadrupole TSQ 7000 LC-MS/MS system with atmospheric pressure chemical ionization (APCI) interface (Finnigan MAT, Bremen, Germany). For APCI, the temperatures of the heated vaporizer and inlet capillary in the nebulizer interface were set to 300°C and 200°C, respectively. The current of the APCI corona discharge needle was set to 5.0 μA, resulting in 4.6 kV needle voltage. Nitrogen served both as sheath (10 l min^{-1}) and auxiliary gas (50 psi). Data acquisition and evaluation were carried out on a Personal DECstation 5000/33 (Digital Equipment, Unterföhring, Germany) and ICIS 8.1 software (Finnigan MAT). HPLC separations were carried out on a Lichrospher 100 NH_2 column (250 × 4 mm, 5 μm, Knauer) using isocratic elution with EtOH/H_2O 96:4 at 0.8 ml min^{-1}. Runs were performed in positive mode. Product ion spectra were available by collision induced dissociation (1.8 mTorr Argon, −15 eV).

2.6. Product isolation

For preparative scale conversion, 100 mg curcumin was dissolved in 40 ml ethanol and poured into 1 l of 0.1 M borate buffer (pH 8.0). After addition of 50 mg of LOX the mixture was stirred for 3 h at ambient temperature with air constantly bubbling through the mixture. The reaction was terminated by adjusting the pH to 4, then solid sodium chloride was added up to saturation. The solution was subsequently extracted with three portions of diethyl ether and ethyl acetate each. The combined, dried (Na_2SO_4) and concentrated extracts were analyzed by HPLC on a Lichrospher 100 NH_2 column. Large scale purification was done on a Lichrospher 100 NH_2 column (250 × 16 mm, 5 μm) using isocratic elution with EtOH/H_2O 90:10 at 5.0 ml min^{-1} flow rate. Chiral phase HPLC was performed on a Ceramospher Chiral

RU-1 column (Shisheido, Japan) by isocratic elution with MeOH at a flow rate of 0.9 ml min^{-1}. For all HPLC separations detection was done at 230 nm. CD-spectra of separated enantiomers were recorded in acetonitrile on a Jasco J-600 spectropolarimeter.

2.7. NMR spectroscopy

The ^{1}H and ^{13}C NMR measurements were carried out on Bruker *Avance* DMX-600 and DRX-500 spectrometers in acetone-d_6. The chemical shifts are referred to $\delta_{TMS} = 0$ ppm. For structure elucidation DEPT, H,H-COSY, H,C-HMQC, H,C-HMBC and phase sensitive 2D NOESY spectra were run. The pulse programs were taken from the Bruker software library.

3. Results

3.1. Spectroscopic studies

The conversion of curcumin **1** by soybean LOX-1 was monitored by the decrease in absorbance at 430 nm in a double-beam spectrophotometer. In preliminary studies, an optimum of pH 8.0 was established. Thus, in a typical assay, 20 μl of curcumin stock solution was dissolved in 2 ml of 0.1 M borate buffer (pH 8.0). The reaction was started adding 10 μl LOX-1 (10 mg protein ml^{-1}) and allowed to proceed for 4 min. UV spectra indicated that the remaining amount of **1** after 4 min was negligible. As the enzymatic reaction was done in the blank cuvette, an increase in absorbance at 430 nm was recorded. Fig. 1 shows the time course of the degradation of **1** at different concentrations (14–68 μM). Quantification was performed using $\varepsilon = 27{,}500\ M^{-1}\ cm^{-1}$. A plot of v vs. $[S]$ showed the typical Michaelis–Menten kinetics as derived with linoleic acid as substrate. K_m and V_{max} values were different from those obtained for linoleic acid (Table 1). K_m for **1** was about four-fold higher than that recorded for linoleic acid; V_{max} was decreased five-fold. No conversion of **1** was observed when heat-inactivated LOX-1 was used.

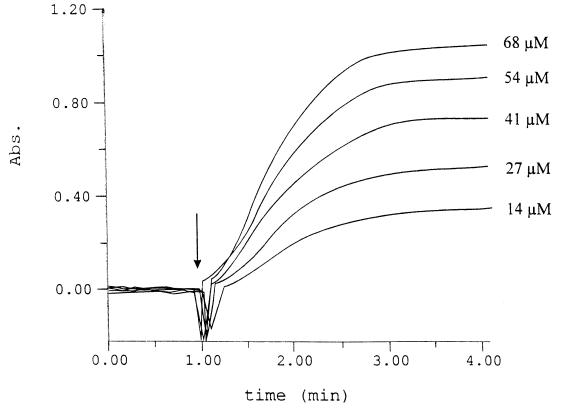

Fig. 1. Time-course (photometric assay) of the decomposition of curcumin **1** by LOX-1; increasing amounts (14–68 μM) of **1** were used as substrate (arrow indicates addition of LOX-1. $\lambda = 430$ nm, 2 ml 0.1 M borate buffer (pH 8.0).

Table 1
Kinetic parameters (K_m, V_{max} and k_{cat}) of LOX-catalyzed oxygenation of curcumin **1** and linoleic acid

Substrate	Assay	K_m (μM)	V_{max} (μM min^{-1})	k_{cat} (s^{-1})
Curcumin	photom.	95	53	2.8
Curcumin	polarogr.	76	36	1.9
Linoleic acid	photom.	20	250	13.3

3.2. Polarographic studies

Oxygen consumption of the enzymatic reaction was monitored in a Clark type oxygen electrode. Different concentrations of **1** (10–100 μg ml^{-1} corresponding to 27–270 μM) were used in this assay. Again, the reaction was started by addition of LOX-1. The rate of oxygen consumption was found to be dependent on the concentration of substrate establishing Michaelis–Menten (first order) kinetics of oxygen insertion. A non-linear regression of the data obtained in this assay revealed 76 μM as K_m and 36 μM min^{-1} as V_{max}. No oxygen consumption was observed when LOX-1 was heat-inactivated prior to reaction. Correlation between the absolute amount of oxygen con-

Table 2
Inhibition of LOX-catalyzed oxygenation of curcumin **1**

Substrate	Inhibitor (concentration (mM))	Assay	Relative reaction rate (%)
Curcumin	–	photom.	100
Curcumin	–	polarogr.	100
Acetylated curcumin	–	polarogr.	19
Curcumin	$HgCl_2$ (1.0)	polarogr.	0
Curcumin	BHA (0.06)	photom.	0
Curcumin	deferoxamine (0.5)	photom.	52
Curcumin	hydroxylamine (8.8)	photom.	0
Curcumin	hydroquinone (1.8)	photom.	18
Curcumin	dithizone (0.2)	photom.	0

sumption (μmol) and the amount of **1** used in the assay (μmol) was linear; the obtained ratio was 0.8 to 1.

When acetylated curcumin ($C_{25}H_{24}O_8$) was used in the polarographic assay, the relative reaction rate was decreased five-fold (Table 2).

3.3. Inhibition experiments

In an additional series of experiments the enzymatic nature of LOX-1 action on **1** was investigated. In order to exclude degradation of **1** by free radicals generated from LOX-1 activity, inhibition of the enzymatic reaction was carried out in the presence of different inhibitors. The photometric assay was allowed to proceed for 1 min after the addition of LOX-1 and was terminated by rapid addition of typical inhibitors (Table 2). Addition of BHA (0.06 mM), hydroxylamine (8.8 mM) and dithizone (0.2 mM) immediately stopped the conversion of **1**, while deferoxamine (0.5 mM) and hydroquinone (1.8 mM) left a relative reaction rate of 52% and 18%, respectively. When 1 mM $HgCl_2$ was present in the polarographic assay, no consumption of oxygen was observed.

3.4. Product isolation and identification

For preparative scale conversion, 100 mg curcumin was oxygenated with LOX-1 and the mixture extracted subsequently. The concentrated extract was analyzed by HPLC on a Dichrospher 100 NH_2 column. A typical run is shown in Fig. 2. As major conversion product **2** was detected. Product **2** was isolated by preparative scale HPLC and further examined by spectroscopic and chromatographic techniques.

Chiral phase HPLC on a Ceramospher Chiral RU-1 column separated compound **2** into two peaks of identical area (Fig. 2, insert). CD spectroscopy of the isolated enantiomers (obtained by multiple injection) yielded two opposite CD spectra which proved metabolite **2** to be a racemic mixture of two enantiomers.

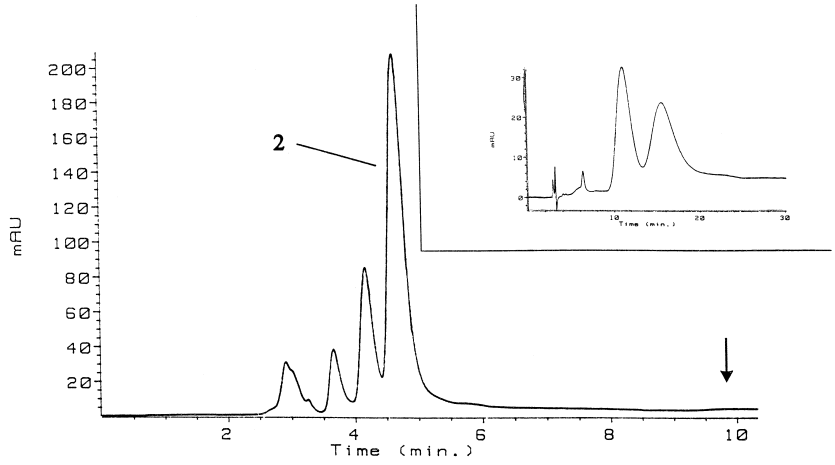

Fig. 2. HPLC chromatogram of products formed by LOX-catalyzed oxygenation of **1**. Elution time of **1** is indicated by the arrow; column: Lichrospher 100 NH_2 (250 × 16 mm, 5 μm, 0.8 ml min^{-1}, EtOH/H_2O 85:15, UV 230 nm). Insert shows separation of **2** by CP-HPLC, Ceramospher Chiral RU-1, 0.9 ml min^{-1}, MeOH, UV 230 nm.

Table 3
^{1}H and ^{13}C chemical shifts (600/125 MHz, acetone-d_6) and J(H,H) coupling constants observed for **2**

No.	δ ^{1}H (ppm)	Multiplicity	Coupling constant (Hz)	δ ^{13}C (ppm)
1	3.63	dd	$J_{1\text{-H},5\text{-H}} = 6.3$/ $J_{1\text{-H},7\text{-H}} = 1.0$	55.8
2	5.90	s	$J_{2\text{-H},1\text{-H}} = 0$	97.9
4	5.41	d	$J_{4\text{-H},5\text{-H}} = 8.2$	80.2
5	3.26	dd	$J_{5\text{-H},1\text{-H}} = 6.3$/ $J_{5\text{-H},4\text{-H}} = 8.2$	54.8
6	–	–	–	200.8
7	4.89	d	1.0	109.4
8	–	–	–	187.9
1′	–	–	–	148.4
2′	6.92	d	2.7	105.4
3′	–	–	–	149.0
4′	–	–	–	145.6
5′	6.87	d	8.6	115.9
6′	6.71	dd	2.7/8.6	112.9
3′-OMe	3.87	s	–	56.4
1″	–	–	–	129.8
2″	6.84	d	1.9	111.5
3″	–	–	–	147.6
4″	–	–	–	146.7
5″	6.69	d	8.1	114.9
6″	6.74	dd	1.9/8.1	120.5
3″-OMe	3.76	s	–	56.1

HPLC-APCI-MS and tandem MS in positive mode of product **2** revealed m/z 401 as molecular adduct ion $[M + H]^+$. Curcumin (MW 368) showed a molecular adduct ion $[M + H]^+$ m/z 369 under the same conditions. So, we concluded a molecular mass of 400 for the metabolite. Tandem MS studies of **2** (product ions of m/z 401, collision energy −15 eV, 1.8 mTorr Ar) yielded the following fragment ions: m/z 401 ($[M + H]^+$), 383 ($[M - H_2O + H]^+$), 355 ($[M - 46 + H]^+$), 277 ($[C_{14}H_{13}O_6]^+$), 259 ($[C_{14}H_{13}O_6–H_2O]^+$) and 249 ($[C_{13}H_{13}O_5]^+$) as base peak.

In the ^{13}C NMR spectrum of **2** 21 signals appeared. DEPT measurement proved the existence of seven =CH, four CH and two MeO units. The five signals between 145 and 150 ppm substantiate five quaternary aromatic sp^2 carbon atoms, which are attached to oxygen atoms. A β-diketone moiety in enolated form is in accordance with the quaternary signals at 200.8 and 187.9, and with δ = CH at 109.4 ppm, the signal of the attached proton appearing at 4.89 ppm (d, 1H). ^{1}H and ^{13}C NMR chemical shifts and characteristic J(H,H) couplings are summarized in Table 3. Similar to **1**, two 1,3,4-trisubstituted aromatic rings can be identified in the product **2**. The NOESY cross-peaks between 2′-H and 3′-MeO, and between 2″-H and 3″-MeO (Table 4), respectively, allowed assignment of the methoxy groups to the different aromatic rings. The HMQC supported the assignment of the aromatic tertiary carbon atoms, while the HMBC measurement unequivocally proved the assignment of the quaternary signals, since the cross-peaks revealed the two- or three-bond correlation between protons and carbon atoms. The connectivities obtained from HMBC between δ3′-MeO at 3.87 ppm and C-3′, furthermore between δ3″-MeO at 3.76 ppm and C-3″ supported their ^{13}C assignment to the signals 149.0 and 147.6, respectively. The cross-peaks of the 5′-H proton delivered δC-3′ and δC-1′ (148.4). The high chemical shift of this carbon atom provides strong evidence that this ring is connected via an oxygen atom to the molecule. The

Table 4
Results from the two-dimensional NMR experiments: ^{1}H and ^{13}C long-range correlations observed by 2D HMBC measurement (600/125 MHz, J(H,C) = 5 Hz) and characteristic proton–proton steric proximities resulted from 2D NOESY measurement (500 MHz, τ_{mix} = 0.5 s) observed for **2**

Proton	^{1}H and ^{13}C long-range correlations (HMBC)	Proton–proton steric proximities (2D NOESY)
	Carbon	NOE observed
1	2; 8	2-H; 4-H; 5-H
2	1; 4; 5; 8	1-H
4	6; 1″; 2″; 6″	5-H; 1-H; 2″-H; 6″-H
5	6; 8	4-H; 1-H
7	1; 5	
2′	1′; 3′; 4′; 6′	3′-OMe
5′	1′; 3′; 4′	
6′	1′; 2′; 4′	
3′-OMe	3′	
2″	4; 3″; 4″; 6″	4-H; 3″-OMe
5″	1″; 3″; 4″	
6″	4; 2″; 4″	4-H
3″-OMe	3″	

assignment of δC-1″ (129.8) is based on the correlation with 5″-H, and its chemical shift indicates the connection of this ring to a carbon atom. The cross-peaks between 4-H and C-2″, and between 4-H and C-6″, respectively, proved that this ring is attached to C-4 (80.2). Considering the downfield appearance of this signal we can conclude that C-4 is connected to an oxygen atom. The strong shielding of C-2 (97.9) is diagnostic for its connection with two oxygen atoms as substituents. The proton–proton cross-peaks observed in the COSY experiment supported the connectivities among 1-H, 4-H and 5-H, but no coupling with 2-H was observable because of J(1-H, 2-H) ~ 0 Hz. The bonding of C-2 to C-1 and O-3, respectively, was determined from HMBC cross-peaks between 2-H and carbon atoms C-1, C-4, C-5 and C-8. On the basis of the long-range C,H connectivities between 2-H and C-8, and furthermore between 4-H and C-6, we concluded that in the β-diketo moiety C-6 appears in keto, C-8 in enol form.

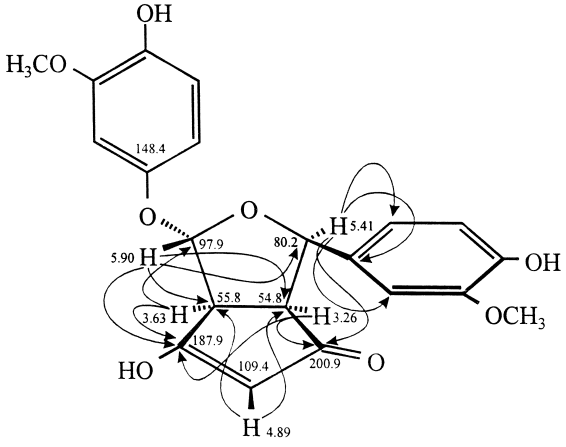

NOESY measurements were used to elucidate the steric arrangement of the substituents of the tetrahydrofuran ring. The results of these measurements are shown in Table 4. The NOE response between 1-H and 4-H proved their *cis* arrangement. The annelation of the two five-membered rings only allows *cis* configuration

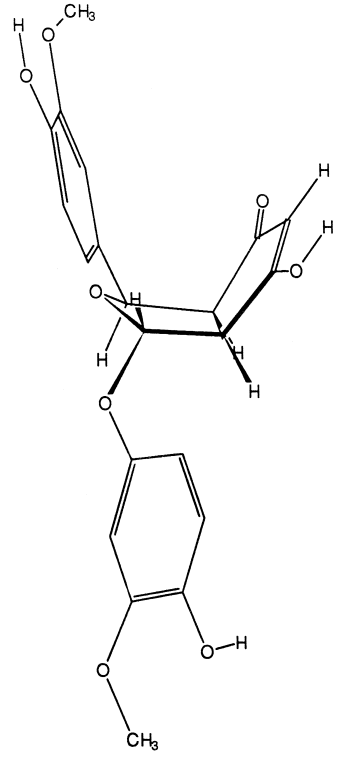

Fig. 3. Three-dimensional structure of **2** as derived by molecular modelling; note: bond angle between H-1 and H-2 is 90°.

for 5-H. 2-H exhibits a NOE cross-peak only with 1-H, which indicates that 2-H should be *trans* situated to 1-H, 4-H and 5-H in the tetrahydrofuran ring. In this case the dihedral angle between 1-H and 2-H is nearly 90°, which is in accordance with the observed J(1-H, 2-H) ~ 0 Hz coupling. On the basis of all chromatographic and spectroscopic data product **2** was identified as a racemic mixture of (1*SR*,2*SR*,4*SR*,5*SR*)-2-[(4′-hydroxy-3′-methoxy)-phenoxy]-4-(4″-hydroxy-3″-methoxy-phenyl)-8-hydroxy-6-oxo-3-oxabicyclo[3.3.0]-7-octene (**2**, $C_{21}H_{20}O_8$). Molecular modelling (Hyperchem 4) was carried out to visualize the stereochemistry of the product. The result is depicted in Fig. 3.

4. Discussion

Our studies revealed **1** as an excellent substrate for LOX-1 despite the lack of a pentadi-

ene system. Spectroscopic and polarographic assays showed rapid conversion of **1** by the enzyme. In neither of the assays degradation of **1** was observed with heat-inactivated LOX-1. Conversion of **1** was immediately stopped by addition of typical LOX-1 inhibitors (which did not act as radical scavengers). These findings clearly demonstrated the enzymatic nature of the reaction. Therefore, we exclude that degradation of **1** was effected by free radicals, as they may be derived during the LOX reaction.

Gardner [2] has presented a pH-dependent head-to-tail mechanism for LOX selectivity indicating that the carboxylic moiety acts as a signal for orientation of the substrate in the active site of the enzyme. Protonation of the carboxylic group leads to decreased hydrophobicity and inverse orientation of the substrate molecule resulting in a lack of regioselectivity. Thus, the carboxylic moiety of a fatty acid acts as signal for the enzyme. We provide evidence that under alkaline conditions the phenolic hydroxyl group of **1** mimics the carboxylate group. Nevertheless, **1** is a symmetric molecule, so there is no regioselectivity to be expected. This view is supported by our data obtained with acetylated curcumin. When both phenolic proups are blocked the enzymatic degradation is significantly slowed down.

Scheme 1 summarizes the formation of **2** by LOX action on curcumin **1**. Major formation of **2** was observed. The structural elucidation of by-products (see Fig. 2) is still under progress. None of the products that arise from chain cleavage as effected by light or alkaline pH [20,21] were detected. Oxygen insertion was confirmed by the MS data of the main product **2** isolated from the reaction mixture. The molecular mass of **2** (M_r 400) is 32 Da higher compared to **1** (M_r 368), which is equivalent to dioxygenation of the substrate. Structure elucidation of **2** was done by extensive NMR analyses. All obtained spectroscopic data proved identity of **2** with (1*SR*, 2*SR*, 4*SR*, 5*SR*)-2-[(4′-hydroxy-3′-methoxy)-phenoxy]-4-(4″-hydroxy-3″-methoxy-phenyl)-8-hydroxy-6-oxo-3-oxa-bicyclo[3.3.0]-7-octene (**2**, $C_{21}H_{20}O_8$). To our knowledge **2** represents a new type of bicyclus that has not been described before.

Markus et al. have reported oxidation of isoeugenol, coniferyl benzoate and analogues by LOX [22]. LOX-mediated cleavage of the double bond adjacent to the substrate's phenolic ring yielded considerable amounts of phenolic aldehydes, e.g., vanillin. The enzymatic reaction, however, was not described as a dioxygenation and remained unresolved. In our experiments, we detected only minor amounts (below 1%) of vanillin as cleavage products.

Hydroperoxides are the major products isolated after LOX action on its common substrates, i.e., 1,4-*Z*,*Z*-pentadienoic fatty acids. Although we were not able to detect any, we assume intermediate formation of a curcumin hydroperoxide, the peroxy group presumably located at C-1 of curcumin (for numbering see Scheme 1). Certainly, such a hydroperoxide should be very unstable and easily undergo rearrangement reactions. Product **2** should arise via rearrangement and migration of the phenolic ring which is a common phenomenon that occurs with, e.g., cumene hydroperoxide. Nonetheless, this explains neither formation of the furanone nor of the attached five-membered

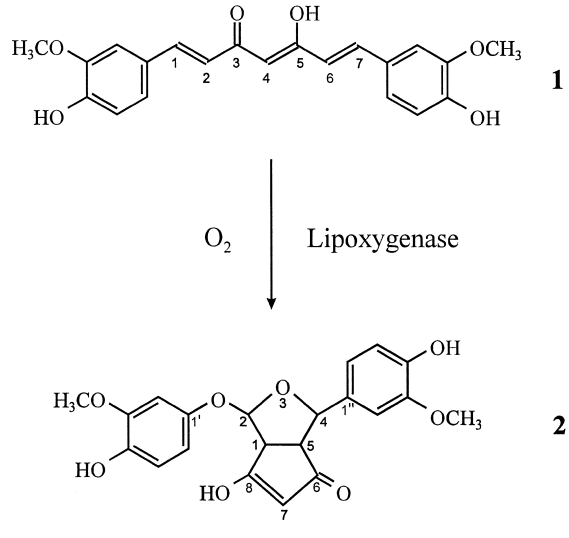

Scheme 1.

ring. Further work is necessary to elucidate the mechanism leading to formation of **2**.

Usually stereospecific abstraction of a proton from the double allylic methylene group of a substrate is the first step in LOX catalysis. Curcumin, despite its lack of an apparent 1,4-*Z,Z*-pentadiene system, is an excellent substrate for soybean lipoxygenase and is oxygenated at a high reaction rate. One may suggest that the 1,3-diketo form of **1** may offer a quasi-double allylic methylene, although we have no experimental evidence for this assumption to date. Furthermore, this tautomer is only to about less than 1% present in curcumin solutions.

Acknowledgements

This work was supported by the DFG (SFB 347) and Fonds der Chemischen Industrie, Frankfurt. Dr. M. Herderich is thanked for the support provided in LC-MS/MS studies. We thank E. Ruckdeschel and Dr. D. Scheutzow from the Institute of Organic Chemistry, Universität Würzburg, for recording some of the NMR spectra.

References

[1] G.A. Veldink, J.F.G. Vliegenthart, Adv. Inorg. Biochem. 6 (1984) 139–161.
[2] H.W. Gardner, Biochim. Biophys. Acta 1084 (1991) 221–239.
[3] H. Kühn, T. Schewe, S.M. Rapoport, Adv. Enzymol. 58 (1986) 273–311.
[4] H. Kühn, L. Eggert, O.A. Zabolotsky, G.I. Myagkova, T. Schewe, Biochemistry 30 (1991) 10269–10273.
[5] A.N. Grechkin, R.A. Kuramshin, S.K. Latypov, Y.Y. Safonova, T.E. Gafarova, A.V. Ilyasov, Eur. J. Biochem. 199 (1991) 451–457.
[6] M.O. Funk Jr., J.C. Andre, T. Otsuki, Biochemistry 26 (1987) 6880–6884.
[7] C.S. Ramadoss, E.K. Pistorius, B. Axelrod, Arch. Biochem. Biophys. 190 (1978) 549–552.
[8] D. Waldmann, P. Schreier, J. Agric. Food Chem. 43 (1995) 626–630.
[9] B. Cohen, S. Grossman, B.P. Klein, A. Pinsky, Biochim. Biophys. Acta 837 (1985) 279–287.
[10] W.F. Hughes, W. Chamulitrat, R.P. Mason, T.E. Eling, Carcinogenesis 10 (1989) 2075–2080.
[11] B. Samuelsson, S.E. Dahlén, J.A. Lindgren, C.A. Rouzer, C.N. Serhan, Science 237 (1987) 1171–1176.
[12] D.C. Zimmerman, C.A. Coudron, Plant Physiol. 63 (1979) 536–541.
[13] B.A. Vick, D.C. Zimmerman, Biochem. Biophys. Res. Commun. 111 (1983) 470–477.
[14] J.N. Siedow, Annu. Rev. Plant Physiol. Plant Mol. Biol. 42 (1991) 145–188.
[15] R.R. Satoskar, S.J. Shah, S.G. Shenoy, Int. J. Clin. Pharmacol. Ther. Toxicol. 24 (1986) 651–654.
[16] K. Mehta, P. Pantazis, T. McQueen, B.B. Aggarwal, Anti-Cancer-Drug 8 (1997) 470–481.
[17] M.T. Huang, T. Lysz, T. Ferraro, T.F. Abidi, J.D. Laskin, A.H. Conney, Cancer Res. 51 (1991) 813–819.
[18] H.H. Tønnesen, Int. J. Pharm. 50 (1989) 67–69.
[19] H.J.J. Pabon, Recl. Trav. Chim. Pays-Bas 83 (1964) 379–386.
[20] H.H. Tønnesen, J. Karlsen, Z. Lebensm. Unters. Forsch. 180 (1985) 132–134.
[21] H.H. Tønnesen, J. Karlsen, G.B. van Henegouwen, Z. Lebensm. Unters. Forsch. 183 (1986) 116–122.
[22] P.H. Markus, A.L.J. Peters, R. Roos (1991) EP 0542348 A2.